

RSC Advances



This is an *Accepted Manuscript*, which has been through the Royal Society of Chemistry peer review process and has been accepted for publication.

Accepted Manuscripts are published online shortly after acceptance, before technical editing, formatting and proof reading. Using this free service, authors can make their results available to the community, in citable form, before we publish the edited article. This *Accepted Manuscript* will be replaced by the edited, formatted and paginated article as soon as this is available.

You can find more information about *Accepted Manuscripts* in the [Information for Authors](#).

Please note that technical editing may introduce minor changes to the text and/or graphics, which may alter content. The journal's standard [Terms & Conditions](#) and the [Ethical guidelines](#) still apply. In no event shall the Royal Society of Chemistry be held responsible for any errors or omissions in this *Accepted Manuscript* or any consequences arising from the use of any information it contains.

25 with fast, economic and nondestructive advantages compared to traditional chemical
26 methods.

27 **Keywords:** *Epimedium*, Fourier transform near-infrared (FT-NIR), Partial least
28 square regression (PLSR), Competitive adaptive reweighted sampling (CARS)

29

30 **1. Introduction**

31 *Epimedium* (Yinyanghuo) is a popular traditional Chinese medicine with a long
32 history in China. Almost fifty varieties *Epimedium* are distributed around the world
33 and twenty-three varieties are found in China, the geographical distribution center
34 of *Epimedium*.¹ Five official species were designated in Chinese Pharmacopoeia,
35 including *Epimedium brevicornum* Maxim., *E. Sagittatum* Maxim., *E. Pubescens*
36 Maxim., *E. Wushanense* T.S. Ying and *E. koreanum* Nakai.² The aerial part is of
37 great value in the treatment of cardiovascular diseases, osteoporosis and
38 improvement of sexual function.²⁻⁵

39 Flavonoids are generally considered as the major active constituents of
40 *Epimedium*, and over 141 flavonoids, including flavone and its derivatives, have
41 been found from 17 *Epimedium* species.⁶ Among them, epimedin A, B, C and
42 icariin, which make up more than 52% of total flavonoids in epimedium, are
43 perceived as major bioactive components.⁷ Four flavonoids exhibit a promising
44 therapeutic efficacy of antitumor, cardiac-cerebral vascular disease, anti-oxidant,
45 antidepressants and antiobesity.^{4, 8, 9} Quantitative and qualitative studies about
46 *Epimedium* have been extensively investigated. Many analytical techniques, such as
47 HPLC,⁷ capillary zone electrophoresis (CZE)¹⁰ and micellar electrokinetic
48 chromatography (MEKC),¹¹ have been applied for the investigation of epimedin A,
49 B, C and icariin simultaneously. However, these methods are time-consuming,

50 laborious and need additional reagents in sample processing. To address these issues,
51 it is necessary to develop new methods for determining the four flavonoids in
52 *Epimedium*.

53 As a rapid, economical and nondestructive analytical technique, FT-NIR
54 spectroscopy has been widely applied in quality evaluation and quality control of
55 food, agriculture, and pharmaceutical products, such as honey,¹² tea¹³ and
56 honeysuckle.¹⁴ It is applied based on molecular overtone and combination
57 vibrations of the fundamental -OH, -CH, and -NH bonds, which are the main
58 recordable phenomena in the radiation region (12500-4000 cm^{-1}) of near-infrared
59 spectrum.¹⁵ However, NIR spectra are often highly correlated due to the strongly
60 overlapped and broad absorption bands,¹⁶ so the data are often calibrated with the
61 classical partial least squares regression (PLSR).^{17, 18} A calibration process on the
62 basis of full-range spectra is time consuming and adverse to fulfilling the high-
63 speed features of NIR spectroscopy. Instead, the selected informative wavelengths
64 instead of full-spectrum can result in a better quantitative calibration model.^{19, 20} Li
65 et al. demonstrated that CARS performed a competitive selection of some key
66 wavelengths which were interpretable to the chemical property of interest, by
67 comparing CARS²¹ with a moving window (MW)²² and a Monte Carlo
68 uninformative variable elimination (MC-UVE)²³ selection method.

69 This study combined CARS with PLSR algorithm to determine epimedin A, B,
70 C and icaniin in *Epimedium*. CARS was applied to select key wavelengths from the
71 full-range of NIRS. The objectives of this work include two aspects: (I) to establish
72 the relationships between the NIR spectroscopy spectra and the content of the four
73 flavonoids, (II) to discuss the benefits of selecting the most informative spectral

74 variable (with CARS-PLSR compared with full spectrum-PLSR) for calibration
75 accuracy and model parsimony.

76

77 **2. Materials and methods**

78 **2.1. Materials and reagents**

79 Seventy-five batches of commercial samples of *Epimedium* were collected
80 from 18 different provinces in China. HPLC-grade acetonitrile (Merck, Darmstadt,
81 Germany), methanol (Hanbang Chemicals, Jiangsu Province, China), dehydrated
82 alcohol (Huihong Chemicals, Hunan Province, China), and phosphoric acid (Kermel,
83 Tianjin, China) were purchased. Deionised water was purified with a Milli-Q system
84 (Millipore, Bedford, MA, USA). Epimedin A, epimedin B, epimedin C and icariin
85 were purchased from Beijing Century Aoke Biotechnology Co. Ltd.

86 **2.2. Sample preparation**

87 The dried aerial parts of the samples, a total of seventy-five batches, were
88 pulverized with small high-speed universal grinder and passed through a 60 mesh
89 sieve. The powdered samples were oven-dried at 65 °C for 4 h according to the
90 reference.⁷ The dried samples were kept in ziplock bags and stored in dark place
91 prior to further analysis.

92 One gram pulverized sample was weighed accurately and mixed with 25 ml 80%
93 ethanol solution in a 100 ml conical flask. The mixture was sonicated for 30 min at
94 the extraction temperature of 40 °C. The supernatant was filtered and the filtrate was
95 collected as the crude extract. The crude extract was transferred to a 250 ml
96 volumetric flask, and adjusted to 250 ml (V_{solution}) with 80% ethanol solution. The
97 solution was filtered through 0.45 µm membranes before HPLC analysis.

98 2.3. HPLC analysis

99 Quantitative analysis of epimedin A, B, C and icariin in *Epimedium* was
100 performed on a Dionex ultimate 3000 series instrument (California, USA), which
101 consists of a binary pump, a diode-array detector (DAD), an automatic injector, an
102 autosampler and a column compartment. The HPLC separation was achieved on a
103 SinoChrom ODS-BP column (5 μ m, 250 mm \times 4.6 mm, Elite, Dalian, China). The
104 mobile phase consisted of (A) 0.1% phosphoric aqueous acid and (B) acetonitrile in
105 a gradient mode as follows: 22-33% (v/v) B at 0-15 min, 33-35.4% B at 15-20 min,
106 35.4-50% B at 20-25 min, 50-50% B at 25-35 min, 50-22% B at 35-37 min, 22% B
107 at 37-40 min. The injection volume was 10 μ L and the flow rate was 1.0 ml/min.
108 The column compartment was kept at 25 °C. DAD detection was accomplished at
109 270 nm. Chromatographic peaks of epimedin A, B, C and icariin were identified
110 according to the retention time and the UV spectrum with the reference standards.
111 The external standard method was applied to quantification of the four flavonoids.

112 2.4. NIR spectral measurement

113 The FT-NIR reflectance spectra were collected using an Antaris II FT-NIR
114 spectrophotometer (Thermo Electron Co., USA) with an integrating sphere. Each
115 spectrum was recorded between 10000 cm⁻¹ and 4000 cm⁻¹ with a resolution of 8
116 cm⁻¹ by co-adding 32 scans and all the spectra were recorded as the logarithm
117 of the reciprocal reflectance, log(1/R). Samples were measure at intervals of 3.856
118 cm⁻¹, and spectrum of each sample had 1557 data points (i.e. spectral variables).
119 About 0.5 g of dry *Epimedium* powder was filled into the sample cup, which was
120 the standard accessory as sample's holder, in the standard procedure. The spectrum
121 of each *Epimedium* sample was collected three times at indoor temperature (25 \pm

122 1) °C. The average of the three spectra collected from the same *Epimedium* sample
123 was used for further analysis.

124 **2.5. Spectral preprocessing**

125 In order to build reliable, accurate and stable models, mathematical spectral
126 pre-treatments to reduce background information and noises beside sample
127 information are necessary. In this work, four data pre-processing methods, including
128 moving window smoothing, multiplicative scattering correction (MSC), standard
129 normal transformation (SNV) and Savitzky-Golay first-derivative (S/G 1st der), and
130 their various combinations were investigated comparatively. Smoothing was applied
131 to modify the magnitude of absorption peaks and shift the position of the
132 asymmetric absorption band. MSC eliminated the effects of the solid scattering on
133 the spectrum. The SNV was a mathematical transformation method which centred
134 and scaled individual spectra. S/G 1st derivative was used to correct baseline effects
135 in spectra.

136 **2.6. Multivariate calibration approach**

137 PLSR analysis is extensively used for multivariate regression in spectroscopic
138 analysis. In PLSR, the spectral data matrix (**X**) and the target chemical properties
139 matrix (**Y**) are considered simultaneously.²⁴ Before the modeling, Kennard and
140 Stone algorithm (K-S),²⁵ which aims at covering the multidimensional space in an
141 uniform manner by maximizing the Euclidean distances between already selected
142 objects and the remaining objects, was applied to selecting calibration set and
143 prediction set.

144 In PLSR model, there are some of spectral variables that contain irrelevant
145 information or noise for modeling **Y**. Eliminating these variables from the pertinent
146 information is conducive to improving the model. In this work, CARS algorithm²¹

147 was used to select the key wavelengths that had large absolute regression
 148 coefficients in PLSR model. In CARS, the first step was to sample in the model
 149 space combined with Monte Carlo strategy. Then, enforced wavelength reduction
 150 and adaptive reweighted sampling (ARS) were employed to remain informative
 151 variables. In enforced wavelength reduction procedure of one variable subset, the
 152 variables were indexed by absolute values of regression coefficients. It was
 153 demonstrated that a large absolute regression coefficient indicates an important
 154 variable in a model.^{26, 27} A number of variables with small absolute regression
 155 coefficients were removed. CARS uses exponentially decreasing function (EDF) to
 156 remove the variables which are less important. In this step, the runs of EDF are set
 157 to N , which means that finding an optimal variable subset would undergo N runs to
 158 iteratively filter the variables with small absolute regression coefficients. In the i th
 159 run of EDF, the number of remaining variables is calculated as follows:

$$160 \quad r_i = pe^{-ki} \quad (1)$$

161 where k is the constant parameter controlling the curve of EDF and p is the total
 162 number of variables. It is related to the curvature of the EDF and has positive
 163 correlation with the speed of the decreasing curve. It is determined by the following
 164 two conditions: (I) when $i = 0$, all the p variables are taken for modeling, which
 165 indicates that $r_0 = p$, (II) when $i = N$, only 2 variables are remained to obtain
 166 $r_N = 2$, where N is the total number of iterations. With the above conditions, k can
 167 be computed as:

$$168 \quad k = \frac{\ln(p/2)}{N} \quad (2)$$

169 where \ln denotes the natural logarithm.

170 Following EDF-based enforced wavelength reduction, ARS was employed in
 171 CARS to further eliminate wavelengths by mimicking the ‘survival of the fittest’

172 principle on which Darwin's evolution theory is based. Finally, 10-fold cross-
173 validation was applied to choose the optimal subset of variables with the lowest root
174 mean square error of cross validation (RMSECV). The performance of the
175 calibration model was evaluated in terms of the RMSE of calibration (RMSEC) and
176 determination coefficient (R^2) for calibration set (R_c^2) in the calibration process. The
177 RMSE of prediction (RMSEP) and determination coefficient (R^2) for prediction set
178 (R_p^2) were used to evaluate the performance of the prediction set in the prediction
179 process. Based on the guideline of Williams,²⁸ R^2 indicates the percentage of the
180 variance in the **Y** variable that is accounted for by the **X** variable. R^2 value greater
181 than 0.90 denotes a good prediction, and 0.82-0.90 is considered to be indicative of
182 a good prediction, whereas 0.66-0.81 indicates an approximate quantitative
183 prediction.

184 **2.7. Data processing**

185 All the codes and computations were written and performed in MATLAB
186 (Version 2013A, the MathWorks, Inc) on a general-purpose computer with Intel(R)
187 Core(TM) i3 2.27GHz CPU and 2GB RAM. The Microsoft Windows 7 was the
188 operating system of the computer. The MATLAB code of data processing is
189 available for academic research in the website:
190 <http://www.mathworks.com/matlabcentral/fileexchange/authors/498750>.

191

192 **3. Results and discussion**

193 **3.1. Content determination by HPLC**

194 A robust HPLC reference method has been established prior to quantitative
195 analysis of epimedin A, B, C and icariin by NIR. Fig. 1 shows the separations of an
196 *Epimedium* extract under the chromatographic condition in section 2.3. Four

197 flavonoids we are concerned are baseline separated. The methodology parameters
198 and calibration curves of the HPLC method were optimized before the real samples
199 analyses, and the results are listed in Table 1. The results of the method validation,
200 including precision, accuracy, linearity and calibration curve, are satisfactory.
201 Therefore, the reference values obtained with this HPLC system are accurate and
202 can be used in subsequent NIR calibration.

203 (Insert Fig.1)

204 (Insert Table 1)

205 3.2. Near infrared spectra

206 Fig. 2 shows the original NIR spectra at wavenumbers 10000-4000 cm^{-1} of 75
207 *Epimedium* samples. It can be found that the intense absorption bands are mainly
208 distributed in the region of 7200-4000 cm^{-1} . In the NIR region, bands around 6876
209 cm^{-1} arise from first overtones of O-H stretching bands¹⁴ while those at 5178 cm^{-1} is
210 due to combination O-H stretching and O-H bending.²⁹ The peaks at 5780 and 5670
211 cm^{-1} are assigned to the first overtone of C-H stretching vibrations of methyl,
212 methylene and ethylene groups.^{30, 31} The O-H and C-H bonds are abundant in the
213 molecular structures of epimedin A, B, C and icariin. The NIR spectra contain the
214 chemical information of interest in *Epimedium* samples sufficiently. However, due to
215 the high degree of band overlap, it is difficult to find the distinct difference in the raw
216 NIR spectra among samples by naked eye. Therefore, it is necessary to introduce
217 chemometric methods to further explore the relationship between the NIR spectra
218 and the internal chemical information.

219 (Insert Fig.2)

220 3.3. Selecting the preprocessing methods

221 Full-spectrum PLSR models were established with different pretreatment
222 methods, including smoothing, MSC, SNV, S/G 1st-der and their various
223 combinations, to reach the minimum RMSEP. The calculated results of calibration
224 and prediction processes are shown in Table 2. As can be seen, in the cases of
225 epimedin A and icariin, the optimal math treatment was SNV, removing slope
226 variations on individual spectrum basis. For epimedin B the best treatment was
227 smooth + MSC. The best treatment for epimedin C was MSC, compensating for
228 different scatter and particle sizes.²⁵ The methods used for different compounds are
229 dissimilar. The reason for this outcome might be that the four flavonoids were
230 related to different effective information of spectral data. Different preprocessing
231 methods reflect the information corresponding to different flavonoids.

232 (Insert Table 2)

233 3.4. Full-spectrum PLSR models

234 Under the condition of optimized spectra pre-treatments, the full-spectrum
235 PLSR models for epimedin A, B, C and icariin were developed. 10-fold cross-
236 validation was applied to the evaluation of the obtained models. The set of
237 calibration samples was divided into 10 subsets for their calibration, of which nine
238 were taken for the calibration set and one for the prediction set. The process was
239 repeated ten times, so that all of the subsets pass through the calibration and
240 prediction set. Fig.3 corresponding to the full-spectrum PLSR models shows the
241 correlation of the values obtained by the reference analysis method and the values
242 predicted by the NIR for epimedin A, B, C and icariin. The red star marked points
243 referred to calibration samples, and the blue round marked points referred to
244 validation samples. The prediction results for prediction set generated by the PLSR

245 models are listed in Table 3. RMSEP were 0.2190, 0.3855, 2.1433, 0.4810 and R_p^2
246 were 0.8566, 0.7139, 0.7360, 0.8789 for epimedin A, B, C and icariin, respectively.
247 Good performance for epimedin A and icariin content determination was achieved
248 by NIR spectra. However, the performance for epimedin B and C was only
249 approximate quantitative predictions, which may be caused by two reasons. For one
250 thing, the relatively poor performance is attributed to the heterogeneity of the
251 sample set, as optimal calibration requires limited but sufficient set heterogeneity.³²
252 For another, the full NIR spectra contain 1557 variables and uninformative variables
253 are included, which lead to the PLSR process complex and affect the predictive
254 performance of calibration models. Thus we proposed CARS to eliminate the
255 uninformative variables prior to application of PLSR.

256 (Insert Fig.3)

257 (Insert Fig.4)

258 (Insert Table 3)

259 3.5. CARS for variable selection

260 As described in Li's previous work,²¹ the number of Monte Carlo sampling
261 runs does not have significant influence on the performance of CARS. Thus, the
262 number of sampling runs was set to 100 as default during the calculation process.
263 During CARS, RMSECV decreased as the wavelengths with more information were
264 retained while other unimportant ones were eliminated. Once any key wavelength
265 was removed, RMSECV value would rise sharply. So the critical point with the
266 lowest RMSECV corresponded to the optimal wavelengths subset, which implied
267 that the valuable information could be retained better only when variables are
268 appropriately reserved. Finally, there were 47, 50, 47 and 44 wavelengths selected
269 for epimedin A, B, C and icariin, respectively. Fig. 5 illustrates the distribution of

270 the selected variables by CARS. It can be seen that the informative wavelengths of
271 all four flavonoids are widely distributed in the wave numbers of 9977-8242 cm^{-1}
272 and 6892-4018 cm^{-1} , which may be seen as a proof for the characteristics of strong
273 overlap, broad absorption bands and high correlation in NIR spectra.¹⁶
274 Simultaneously, the wavenumbers selected for epimedin A, B and C are similar,
275 while the ones corresponding to icariin is somewhat different. This phenomenon
276 may be on account that the structure of icariin is, to some extent, differ from
277 epimedin A, B and C. Epimedin A, B and C have more structural similarity. It
278 indicates that CARS has the ability to effectively extract informative variables
279 relevant to the four different flavonoids from NIR spectra.

280 (Insert Fig.5)

281 CARS-PLSR models for 4 flavonoids were developed under the conditions of
282 the most appropriate wavelengths selected by CARS and the same optimized
283 spectra pre-treatments corresponding to PLSR models. The results of the CARS
284 models are shown in Table 3 and Fig.4. Through comparison of the full-spectrum
285 PLSR models with CARS-PLSR ones, it is clearly showed that the irrelevant
286 variables can be removed effectively and the predictive precision can be improved
287 markedly by CARS method. RMSEP decreased from 0.2190, 0.3855, 2.1433 and
288 0.4810 to 0.1789, 0.2572, 1.2872 and 0.3615; R_p^2 increased from 0.8566, 0.7139,
289 0.7360 and 0.8789 to 0.8969, 0.8810, 0.9273 and 0.9325 for epimedin A, B, C and
290 icariin, respectively. After using the key variables, the performance for epimedin C
291 obtain the most obvious improvement from an approximate quantitative prediction
292 to an excellent prediction, followed by epimedin B. At the same time, one can see
293 that the performance for epimedin C and icariin were improved to excellent
294 predictions and superior to epimedin A and B. The reason may be that the contents

295 of epimedinin A and B are too low (epimedinin A 0.0355-3.1552 mg/g, epimedinin B
296 0.044-5.3131 mg/g), and it is difficult to measure more accurately. In general, the
297 results proved that CARS method could obtain more accurate and parsimonious
298 model for determination of epimedinin A, B, C and icariin in *Epimedium* using NIR
299 spectroscopic methods.

300

301 **4. Conclusions**

302 A FT-NIR method was developed to determine the epimedinin A, B, C and
303 icariin in *Epimedium* with a HPLC-DAD method as the reference method. After the
304 removal of the irrelevant variables in the original NIR spectra, more efficient and
305 parsimonious models based on CARS-PLSR were obtained compared with the full-
306 spectrum PLSR ones. The good performance of CARS-PLSR models showed a
307 potential application of CARS on rigorously selecting NIR informative variables. It
308 can be concluded from the overall results that NIR spectroscopy combined with
309 PLSR is a rapid and nondestructive method for the determination of epimedinin A, B,
310 C and icariin in *Epimedium*. However, more work has to be done, in order to
311 improve the accuracy and robustness of the models, especially for epimedinin A and
312 B.

313

314 **Acknowledgement**

315 The authors gratefully thank National Natural Science Foundation of China for
316 support of the projects (No. 21175157 and 21375151), China Hunan Provincial
317 science and technology department for support of the project (No. 2012FJ4139) and
318 Central South University for special support of the basic scientific research project
319 (No. 2010QZZD007).

320 **References**

- 321 1. L. X. Zhang, Z. M. Zhang, J. H. Huang, Y. S. Jin and H. M. Lu, *Anal. Methods*,
322 2013, **5**, 5331-5338.
- 323 2. Chinese Pharmacopoeia Commission, *Chinese Pharmacopoeia I.*, Chemical
324 Industry Press, Beijing, 2005, p. 229.
- 325 3. M. N. Makarova, O. N. Pozharitskaya, A. N. Shikov, S. V. Tesakova, V. G.
326 Makarov and V. P. Tikhonov, *J. Ethnopharmacol.*, 2007, **114**, 412-416.
- 327 4. X. Zhang, Y. Li, X. Yang, K. Wang, J. Ni and X. Qu, *Life Sci.*, 2005, **78**, 180-186.
- 328 5. F. H. Meng, Y. B. Li, Z. L. Xiong, Z. M. Jiang and F. M. Li, *Phytomedicine*, 2005,
329 **12**, 189-193.
- 330 6. H. Ma, X. He, Y. Yang, M. Li, D. Hao and Z. Jia, *J. Ethnopharmacol.*, 2011, **134**,
331 519-541.
- 332 7. H. Zhang, T. Yang, Z. Li and Y. Wang, *Ultrason. Sonochem.*, 2008, **15**, 376-385.
- 333 8. Y. Li, Z. Xiong and F. Li, *J. Chromatogr. B*, 2005, **821**, 235-239.
- 334 9. T. Z. Liu, C. Y. Chen, S. J. Yiin, C. H. Chen, J. T. Cheng, M. K. Shih, Y. S. Wang
335 and C. L. Chern, *Food Chem. Toxicol.*, 2006, **44**, 227-235.
- 336 10. J. J. Liu, S. P. Li and Y. T. Wang, *J. Chromatogr. A*, 2006, **1103**, 344-349.
- 337 11. S. F. Wang, Y. Q. Wu, Y. Ju, X. G. Chen, W. J. Zheng and Z. D. Hu, *J.*
338 *Chromatogr. A*, 2003, **1017**, 27-34.
- 339 12. O. Escuredo, M. C. Seijo, J. Salvador and M. I. Gonzalez-Martin, *Food Chem*,
340 2013, **141**, 3409-3414.
- 341 13. Q. S. Chen, J. W. Zhao, X. Y. Huang, H. D. Zhang and M. H. Liu, *Microchem. J.*,
342 2006, **83**, 42-47.
- 343 14. W. L. Li, Y. F. Wang and H. B. Qu, *Vib. Spectrosc.*, 2012, **62**, 159-164.
- 344 15. X. Wei, N. Xu, D. Wu and Y. He, *Food Bioprocess Tech*, 2013, **7**, 184-190.
- 345 16. M. Blanco, J. Cruz and M. Bautista, *Anal. Bioanal. Chem*, 2008, **392**, 1367-1372.
- 346 17. M. Vohland, M. Ludwig, S. Thiele-Bruhn and B. Ludwig, *Geoderma*, 2014, **223-**
347 **225**, 88-96.
- 348 18. J. Li, Y. Jiang, Q. Fan, Y. Chen and R. Wu, *Spectrochim. Acta A*, 2014, **125**, 278-
349 284.
- 350 19. D. Wu, X. Chen, P. Shi, S. Wang, F. Feng and Y. He, *Anal. Chim. Acta*, 2009, **634**,
351 166-171.
- 352 20. Y. H. Yun, Y. Z. Liang, G. X. Xie, H. D. Li, D. S. Cao and Q. S. Xu, *Analyst*, 2013,
353 **138**, 6412-6421.
- 354 21. H. Li, Y. Liang, Q. Xu and D. Cao, *Anal. Chim. Acta*, 2009, **648**, 77-84.
- 355 22. B. W. M. Daszykowski, D.L. Massart, *Anal. Chim. Acta*, 2002, **468**, 91-103.
- 356 23. Q. J. Han, H. L. Wu, C. B. Cai, L. Xu and R. Q. Yu, *Anal. Chim. Acta*, 2008, **612**,
357 121-125.
- 358 24. F. Chauchard, R. Cogdill, S. Roussel, J. M. Roger and V. Bellon-Maurel,
359 *Chemometr. Intell. Lab.*, 2004, **71**, 141-150.
- 360 25. R. D. M. A. Candolfia, D. Jouan-Rimbaud, P.A. Hailey, D.L. Massart, *J. Pharm.*
361 *Biomed. Anal.*, 1999, **21**, 115 - 132.
- 362 26. Y.-H. Yun, D.-S. Cao, M.-L. Tan, J. Yan, D.-B. Ren, Q.-S. Xu, L. Yu and Y.-Z.
363 Liang, *Chemometr Intell Lab*, 2014, **130**, 76-83.
- 364 27. D. J.-R. A. Garrido Frenicha, D. L. Massartb, S. Kuttatharmmakulb, M. Martinez
365 Galeraa and J. L. Martinez VidaP, *Analyst*, 1995, **120**, 2787-2792.
- 366 28. W. P.C., *PDK Grain, Nanaimo, Canada*, 2003.
- 367 29. D. Cozzolino, I. Murray, A. Chree and J. R. Scaife, *LWT-Food Sci. Technol.*, 2005,
368 **38**, 821-828.
- 369 30. N. Sinelli, L. Cerretani, V. D. Egidio, A. Bendini and E. Casiraghi, *Food Res. Int.*,
370 2010, **43**, 369-375.
- 371 31. W. L. Li, L. H. Xing, Y. Cai and H. B. Qu, *Vib. Spectrosc.*, 2011, **55**, 58-64.

- 372 32. L. Cécillon, B. G. Barthès, C. Gomez, D. Ertlen, V. Genot, M. Hedde, A. Stevens
373 and J. J. Brun, *Eur. J. Soil Sci.*, 2009, **60**, 770-784.

374

375 **Tables**376 **Table 1**

377 Methodology parameters and calibration curves of the HPLC method.

Compound s	Retention time (min)	Calibration curves	R	Linear range ($\mu\text{g/ml}$)	Limit of detection ($\mu\text{g/ml}$)	Repeatability (RSD%, n=6)	Recovery (%, n=3)
Epimedin A	16.15	$y=16.392x-3.2226$	0.9999	0.25-80	0.013	0.11	105
Epimedin B	16.84	$y=19.838x-3.0745$	0.9999	0.28-120	0.007	0.11	108
Epimedin C	17.37	$y=20.607x-3.5987$	0.9999	0.50-250	0.005	0.16	90
Icariin	18.39	$y=23.581x-5.7396$	0.9999	0.25-250	0.004	0.13	92

378

379

380

381 **Table 2**

382 Optimization of spectral pretreatments in the calibration models of the four
 383 flavonoids.

		MSC	SNV	Smooth + MSC	Smooth + SNV	MSC+S/G 1d	SNV+S/G 1d
	RMSEC	0.1031	0.1307	0.0979	0.1216	0.0486	0.0596
Epimedin	R_c^2	0.9818	0.9715	0.9836	0.9753	0.9961	0.9940
A	RMSEP	0.2214	0.2190	0.2759	0.2568	0.2700	0.2609
	R_p^2	0.8790	0.8566	0.8120	0.8029	0.8065	0.8278
	RMSEC	0.1044	0.1034	0.1785	0.1872	0.1836	0.1882
Epimedin	R_c^2	0.9909	0.9912	0.9734	0.9710	0.9731	0.9715
B	RMSEP	0.3999	0.4302	0.3901	0.3855	0.4387	0.4628
	R_p^2	0.7166	0.6435	0.7303	0.7139	0.5106	0.4852
	RMSEC	0.4417	0.5509	0.5706	0.5084	0.3370	0.7789
Epimedin	R_c^2	0.9904	0.9850	0.9840	0.9873	0.9948	0.9723
C	RMSEP	2.1433	2.3207	2.3316	2.5840	2.5263	2.2491
	R_p^2	0.7360	0.6905	0.6875	0.6162	0.4221	0.5406
	RMSEC	0.3725	0.1987	0.2369	0.3426	0.3255	0.3200
Icariin	R_c^2	0.9567	0.9878	0.9825	0.9638	0.9671	0.9684
	RMSEP	0.7065	0.4810	0.5680	0.5518	0.8590	0.8405
	R_p^2	0.7541	0.8789	0.8410	0.8406	0.6466	0.6408

384

385

386 **Table 3**

387 Statistics of estimates from NIRS using either full spectra-PLS regression or CARS-
 388 PLS regression.

Flavonoids	nLVs ^a	nVAR ^b	Calibration set (N=60)		External validation set (N= 15)	
			R _c ²	RMSEC	R _p ²	RMSEP
Full spectrum-PLS regression						
Epimedin A (mg/g)	16	1557	0.9715	0.1307	0.8566	0.2190
Epimedin B (mg/g)	18	1557	0.9710	0.1872	0.7139	0.3855
Epimedin C (mg/g)	18	1557	0.9904	0.4417	0.7360	2.1433
Icariin (mg/g)	18	1557	0.9878	0.1987	0.8789	0.4810
CARS-PLS regression						
Epimedin A (mg/g)	12	47	0.9567	0.1441	0.8969	0.1789
Epimedin B (mg/g)	16	50	0.9559	0.1001	0.8810	0.2572
Epimedin C (mg/g)	14	47	0.9517	0.5295	0.9273	1.2872
Icariin (mg/g)	11	44	0.9426	0.2655	0.9325	0.3615

389

390 ^a nLVs denotes the number of latent variables.391 ^b nVAR stands for the number selected variables

392

Figure Captions

393

394

395 Fig.1. Representative HPLC-DAD chromatogram at optimized conditions (the
396 peaks marked with 1-4 were epimedin A, B, C and icariin, respectively).

397

398 Fig.2. NIR spectra of the *Epimedium* samples ($N=75$).

399

400 Fig.3. Correlation diagrams between the NIR predicted values based on full spectra-
401 PLSR and the reference values of the flavonoids content (a, b, c, d represent
402 epimedin A, B, C and icariin, respectively).

403

404 Fig.4. Correlation diagrams between the NIR predicted values based on CARS-
405 PLSR and the reference values of the flavonoids content (a, b, c, d represent
406 epimedin A, B, C and icariin, respectively).

407

408 Fig.5. Position of the identified key wavenumbers in the NIRS of *Epimedium*
409 (spectrum averaged from 75 samples and scaled for illustration); a, b, c, d stand for
410 epimedin A, B, C and icariin, respectively.

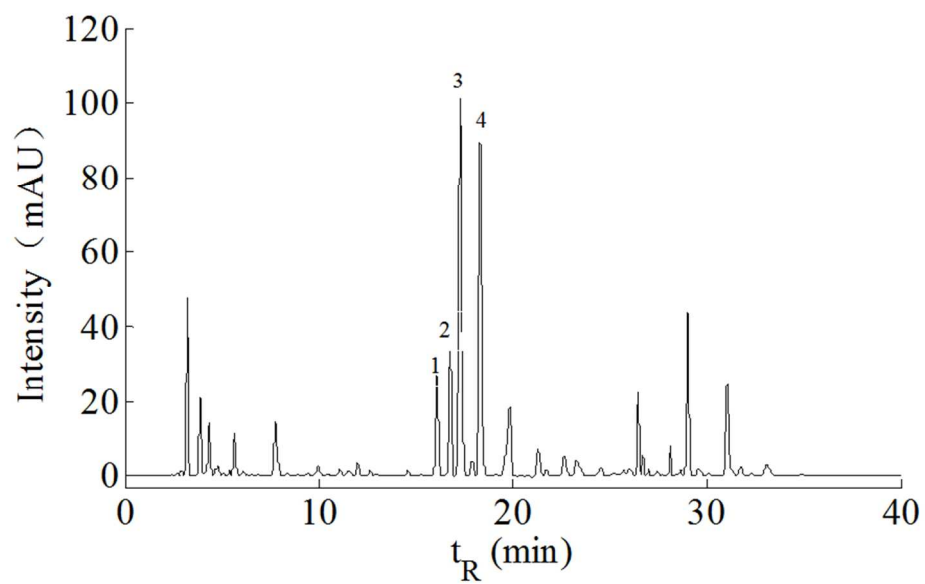


Fig.1. Representative HPLC-DAD chromatogram at optimized conditions (the peaks marked with 1-4 were epimedin A, B, C and icariin, respectively).
253x154mm (96 x 96 DPI)

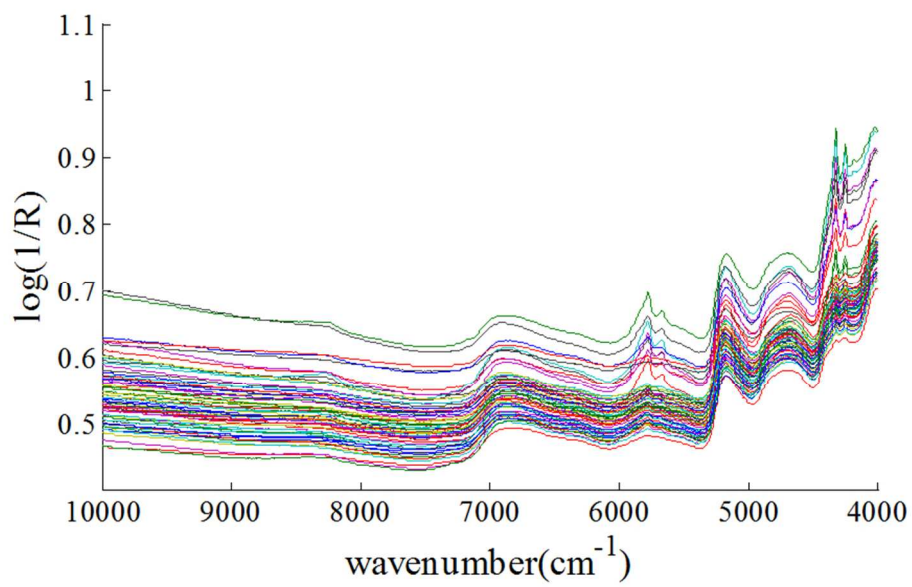


Fig.2. NIR spectra of the Epimedium samples (N=75).
253x154mm (96 x 96 DPI)

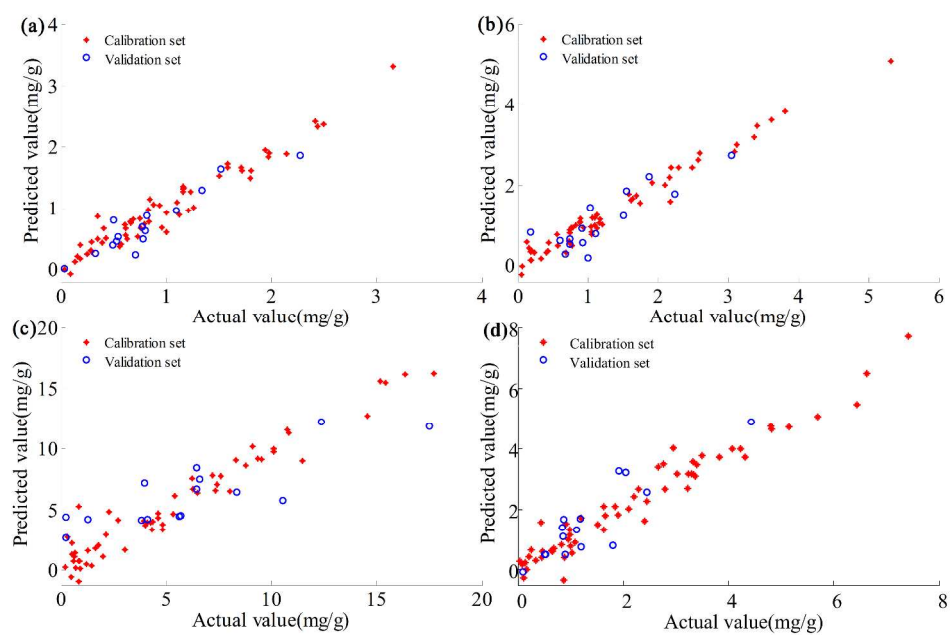


Fig.3. Correlation diagrams between the NIR predicted values based on full spectra-PLSR and the reference values of the flavonoids content (a, b, c, d represent epimedin A, B, C and icariin, respectively).
466x296mm (300 x 300 DPI)

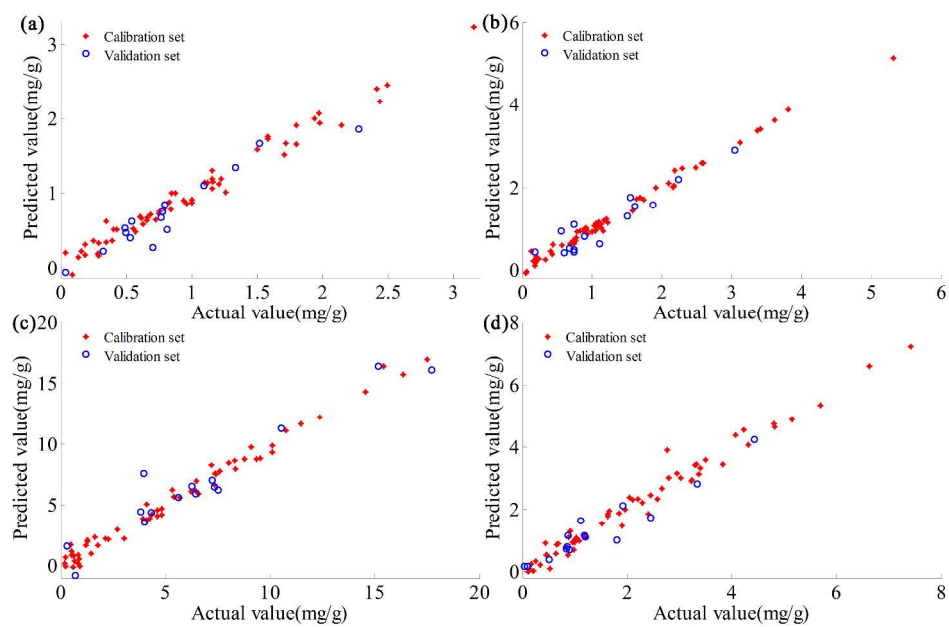


Fig.4. Correlation diagrams between the NIR predicted values based on CARS-PLSR and the reference values of the flavonoids content (a, b, c, d represent epimedin A, B, C and icariin, respectively).
469x295mm (300 x 300 DPI)

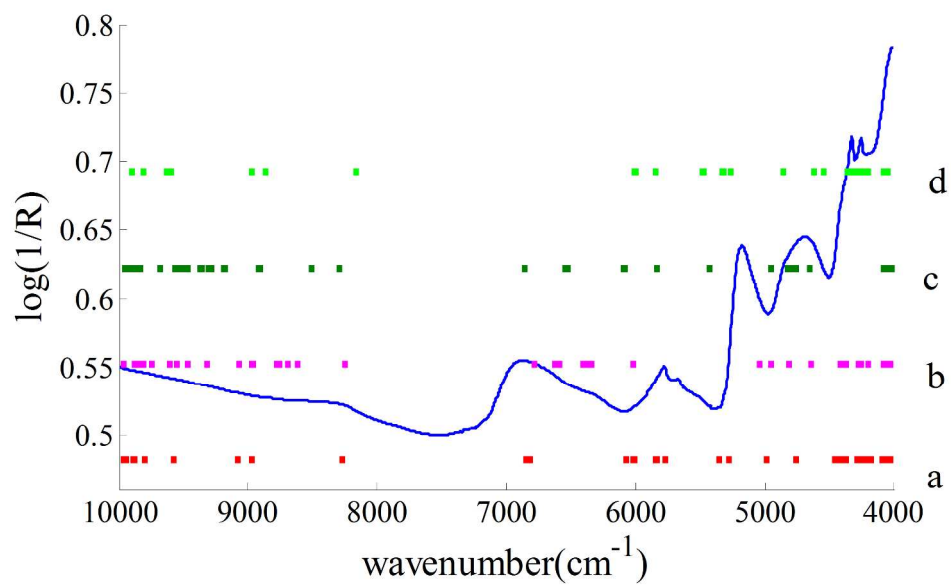


Fig.5. Position of the identified key wavenumbers in the NIRS of Epimedium (spectrum averaged from 75 samples and scaled for illustration); a, b, c, d stand for epimedin A, B, C and icariin, respectively.
253x154mm (300 x 300 DPI)